DEVELOPMENT OF A CONSISTENT DESIGN CONCEPT FOR COMPOSITE DOWELS

Yannick Broschart*, Wolfgang Kurz**, Kevin Wolters***, Georgios Christou***, Markus Feldmann***, Josef Hegger*** and Martin Claßen***

* BORAPA Ingenieurgesellschaft mbH
e-mail: broschart@borapa.de

** University of Kaiserslautern, Germany
e-mail: wolfgang.kurz@bauing.uni-kl.de

*** RWTH Aachen University, Germany
e-mails: k.wolters@stb.rwth-aachen.de, gchristou@imb.rwth-aachen.de,
feldmann@stb.rwth-aachen.de, jhegger@imb.rwth-aachen.de,
mclassen@imb.rwth-aachen.de

Keywords: Composite Dowels, Design Concept, Technical Specification.

Abstract. *Composite dowels are an economically and technically reasonable alternative to the conventional shear connectors, the headed studs. However, their competitiveness is limited by the fact that they are only approved nationally and for a limited period of time, whereas headed studs are firmly anchored in European regulations. Numerous investigations, performed on a national and international level for decades, were necessary in order to enable an integration of composite dowels into the European standards. This paper summarizes the extensive investigations on the influence of cracked concrete, of tensile and combined shear-tensile loads as well as of composite dowel positions close to the surface on the load-bearing behaviour of composite dowels. Based on these and former investigations, a consistent design concept for composite dowels was developed, which will also be presented within this paper and shall form the basis for the introduction into European standardization.*

1   INTRODUCTION AND STATE OF THE ART

Composite dowels for the transfer of longitudinal shear forces between steel cross sections and concrete slabs have several advantages compared to conventional shear connectors, i.e. headed studs. In addition to increased material efficiency [1-3] and corresponding lower CO_2 emissions, structural components with composite dowels are characterized by a simple manufacturing process. Both the flame cutting process and the welding of the composite dowel strips can be automated [4]. In addition, no special welding qualification or equipment is required in contrast to the welding of headed studs according to [5], which also enables small and medium-sized companies to manufacture such steel beams. The use of composite dowels also offers the advantage of high flexibility, as the dowel geometries can be adapted to the specific requirements of the component. This way, high resistance, stiffness and deformability can be achieved, even when using high-strength materials [6].

Composite dowels have been used more and more frequently in recent years, mostly in bridge construction. Nevertheless, in building construction, the market shares of these innovative shear connectors have been extremely low. In addition to the lack of experience of the engineering offices, their competitiveness is also limited by the fact that they are only approved nationally and for a limited period of time [7], whereas headed studs are firmly anchored in European regulations [8]. In Germany the load-bearing capacity per dowel is determined on the basis of a national technical approval via the minimum of

the failure modes steel failure [9], shearing of the concrete dowel [6,7] and pry-out of a concrete cone [10-12]. Under cyclic loading, steel resistance is calculated with the help of the structural stress concept [7,13] and the concrete resistance by means of a stress limitation [7,14]. In this case, further tests are continuously being performed to increase the efficiency of composite dowels [13,15-17].

In order to improve their competitiveness, extensive experimental and numerical investigations were carried out within a joint research project of the RWTH Aachen University and the University of Kaiserslautern, which focused on the corresponding load cases and relevant installation positions in building construction and are shown schematically in figure 1. The aim of the research project was to develop a consistent design concept for composite dowels. This should serve as a basis for the preparation of a CEN Technical Specification. This article summarizes the test program of the small-size specimens within the research project as well as the resulting design model including the underlying engineering models. A more detailed description of individual topics has already been given in [18-20]. Furthermore, large-size component tests were carried out to verify the transferability of the design equations which are presented within the final report [21].
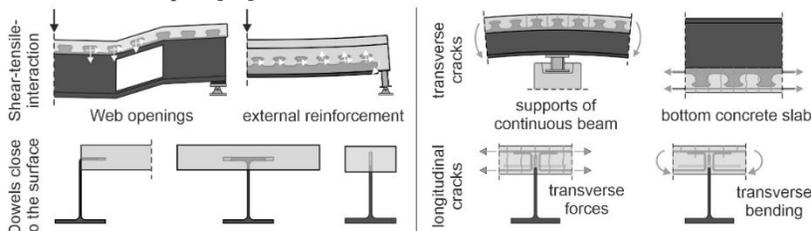

Figure 1. Schematic overview of the examined load situations and installation positions.

2   SHEAR-, TENSION- AND SHEAR-TENSION-RESISTANCE

2.1 General

While the longitudinal shear resistance of composite dowels in non-cracked concrete has already been researched extensively and is regulated within the current German approval, neither their tension- nor their combined shear-tension-resistance is covered in regulations. However, there are conceivable applications where composite dowels are stressed by corresponding loads, for example at the edge of large web openings in steel girders. Within the joint research project, numerous shear-, tension- and shear-tension-tests were performed on single-push-out tests in order to derive an approach for the interaction of both resistances. Furthermore, the calculation of the longitudinal shear-resistance in the current German approval does not consider the influence of concrete cracks. In past research projects [20,22-24], however, a significant reduction of the load-bearing capacity was observed as a consequence of transversal cracks in the concrete slab. In building construction, transversal cracks above central supports of continuous beams, longitudinal cracks above the composite dowels from transversal bending as well as crack formation due to constraining loads in statically indeterminate systems occur. In the research project the resistance of individual dowels in concrete with transversal and longitudinal cracks under shear-, tension- and shear-tension-loads was tested.

2.2 Tension-resistance of composite dowels

The existing approach of the tensile-resistance of composite dowels according to [25-28] was calibrated on small-size tests with puzzle-shaped dowels (PZ) and a uniform embedment depth of 30 mm. In addition, different test series with various dowel geometries (figure 1), embedment depths and positions of the reinforcement bars were performed. The experimental investigations were accompanied by numerical parameter studies.

Figure 2 summarizes the test setup and selected results of the tensile tests based on the *DV* test series (variation of dowel geometry). The specimens were placed centrally under the test cylinder and back-anchored via linear supports parallel to the steel plate (figure 2a). Despite different dowel geometries, the test results were similar with regard to the force-slip curve and the maximum load-bearing capacity (figure 2b). The failure mechanism was usually a large-area concrete pry-out, which settled from the outer edges of the dowel and spread along the stirrup reinforcement (figure 2c+d). In tests with PZ geometry and an arrangement of the reinforcement outside of the steel tooth undercut, the dowels were pulled out without such a large-area failure. On the contrary, the concrete was sheared only in the small undercut areas. This failure at a low load level has to be avoided by a tightly fitting dowel reinforcement in the case of composite dowels under tensile loads.
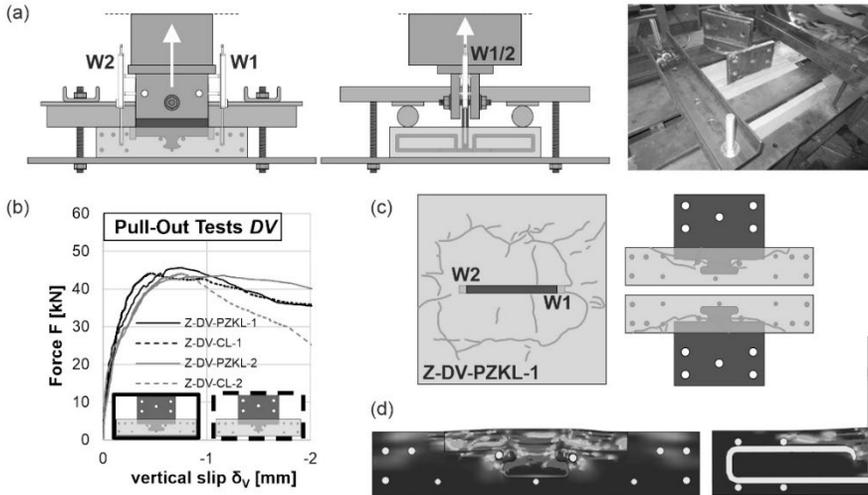

Figure 2. Investigations on the tensile strength of composite dowels, exemplified by the *DV* test series with variation of the dowel geometry (height 40 mm; embedment depth 30 mm): (a) test setup; (b) force-slip curves; (c) crack pattern and pry-out cone; (d) pry-out in numerical parameter studies, representation via the concrete tensile damage in the FE software Abaqus.

2.3 Shear-tension-resistance of composite dowels

In [29], a load introduction construction with varying angles was used to carry out single-push-out tests under combined shear- and tensile-loads. This test setup was used to expand the experimental database within the research project (figure 3, [20]). The influence of the reinforcement arrangement, which had previously been identified as decisive, was systematically investigated. Furthermore, different dowel geometries under five different load angles were considered. The resistance of the examined composite dowels decreased both with increasing distance of the transversal reinforcement from the steel tooth and with increasing angle of load application (increasing tensile component). The position of the transversal reinforcement was only negligible under predominantly shear loads (angle of application <22°). Furthermore, the influence of transversal cracks was systematically investigated in pure tension- and interacting shear-tension-tests. Both the materials used and the measuring techniques are documented in detail in [20].
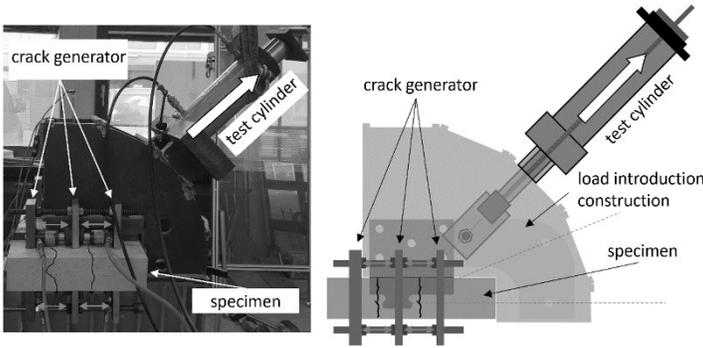
Figure 3. Test setup for shear-tension interaction tests in transversally cracked concrete.

2.4 Small-size tests with longitudinally cracked concrete

The effects of longitudinal cracks in concrete were investigated on the basis of 14 small-size tests, in which both shear- and tensile-loads were applied with different crack widths on otherwise identical test specimens. For this purpose, test specimens with recesses according to figure 4a were used to push both halves of the specimen away from each other by small hand cylinders and threaded rods in order to create longitudinal cracks (figure 4d). The influence of different crack widths on the shear resistance of composite dowels was determined by means of seven tests (figure 4b). Despite high pre-damage due to the crack insertion, no significant reduction of resistance could be observed in comparison to composite dowels in non-cracked concrete. The limiting effect of transversal cracks on pry-out cones does not exist in the case of central longitudinal cracks, as they certainly cross the pry-out cone but do not reduce its shell surface. However, a clear influence of the pre-damage was shown in the tensile tests (figure 4c). Here three different dowel geometries and the influence of transversal reinforcement were tested. In the case of these tests on composite dowels with PZ shape under tensile stress in combination with a central longitudinal crack (with or without transversal reinforcement) pull-out failure occurred. This failure, which strictly has to be avoided, does not emerge in the case of dowel geometries with larger undercuts (CL or PZKL). In the tests with longitudinal cracks in combination with CL or PZKL geometry, a reduction of the resistance could nevertheless be observed, compared to the tests with non-cracked concrete. As a consequence, systematic tensile loads in the area of wide longitudinal cracks should be avoided as far as possible.
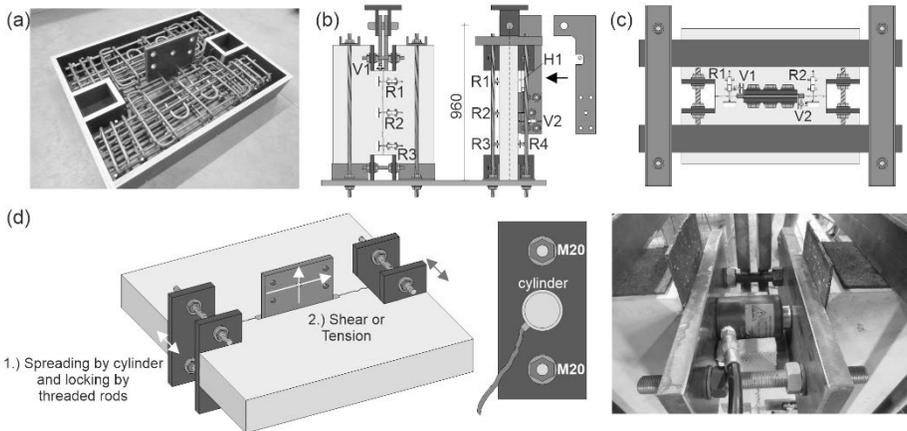

Figure 4. Small-size tests with longitudinally cracked concrete; a) formwork and reinforcement of the test specimens with recesses; b) setup of the shear- or c) tensile-tests; d) crack initiation: bracing of the test specimen halves by spreading plates with the help of hand cylinders and threaded rods.

3 COMPOSITE DOWELS POSITIONED CLOSE TO THE SURFACE

3.1 General

Specifically, in building construction, modern composite structures are being realized increasingly slimmer. To achieve such low slab thicknesses, the composite dowels can be positioned horizontally within the concrete slab (rotated by 90° around their longitudinal axis). In this case, as well as with installation positions close to the free edge of the concrete slab, forms of failure can occur which are not explicitly considered in current regulations, but which are often decisive for the design of slim composite structures. The positions described are referred to as 'close to the surface'. The typical failure mode of composite dowels positioned close to the surface occurs in the form of spalling of the concrete cover and is called edge failure. A horizontal arrangement of the composite dowels allows concrete slab thicknesses far below the limit of $b_c \geq 250$ mm, which is the current restriction of the German technical approval and causes economic disadvantages of the construction method in the field of building construction.

3.2 Small-size tests

In total, more than 40 small-size tests were carried out and accompanied by numerical simulations within the research project to investigate the influence of individual parameters on the load-bearing and deformation behaviour of composite dowels positioned close to the surface. Correspondingly, the influence of the lateral concrete cover $c_{D,s}$, the dowel geometry (PZ, CL or PZKL), the scaling factor e_x, the steel tooth axial spacing, the steel plate thickness t_w, the concrete compressive strength f_c and the arrangement of the transversal reinforcement were inspected. The tests were mainly manufactured in the form of push-out tests with four composite dowels each (figure 5a+b). The force-slip behaviour of specimens with a concrete slab thicknesses b_c of 100 mm, 150 mm and 200 mm is exemplarily shown in figure 5c, while two test specimens of identical parameter configuration were tested in each case. The lateral concrete cover is equal to $c_{D,s} = (b_c - t_w)/2$. Although the maximum load-bearing capacity increased with growing slab thickness, a reduction in stiffness was recorded in all tests at a load level of approximately 265 kN (figure 5c, Detail A). This observation is caused by two overlapping effects.
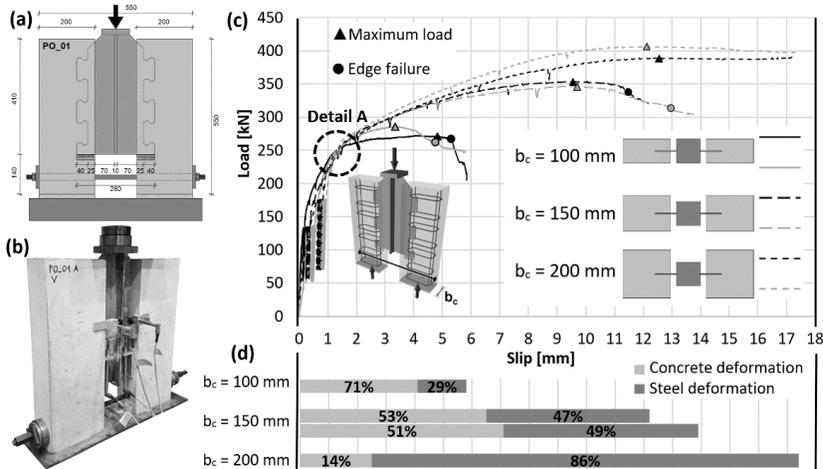
Figure 5. Small-size tests with composite dowels positioned close to the surface: (a) push-out test specimen; (b) test setup; (c) force-slip behaviour with different concrete slab thicknesses b_c; (d) slip composition.

Firstly, it is due to the pulverization of the concrete in the quasi-hydrostatic compressive stress zone directly below the steel teeth, which is also reflected in the predominant concrete deformation in the slip composition of the 100 mm thick specimens (figure 5d) and was described more detailed in [18,19]. Secondly, the 4 mm thick steel teeth reached their yield strength at the said load level, resulting in the large

total slip of the 200 mm thick specimens, their load-bearing capacity was ultimately limited by the steel resistance and not by edge failure. Although concrete pulverization occurred there below the steel teeth, too, the greater lateral concrete cover was sufficient to dissipate the radiating compressive forces. Overall, the ratio of concrete deformations decreased with higher concrete slab thicknesses, while steel tooth deformations increased.

4 ENGINEERING MODELS

4.1 General

Based on the results of the small-size tests, engineering models were developed which were then statistically calibrated on own and former small-size tests according to Annex D.8 of Eurocode 0 [30]. Subsequently, the approaches for tensile- and combined shear-tensile-resistance, transversal cracks and composite dowels positioned close to the surface will be described. The statistically validated equations will be compiled in chapter 5 within a consistent design concept for composite dowels with geometries as shown in figure 6. The longitudinal shear resistance which is currently regulated within the German approval [7] is also proposed to be modified by a new statistical evaluation.

Figure 6. Composite dowel geometries PZ, CL und PZKL.

4.2 Approach to consider the tensile-resistance

To achieve a consistent design concept, the engineering model of the tensile resistance of composite dowels was set up analogously to the pry-out failure mode in case of longitudinal shear loads, where concrete spalling occurs due to a vertical force component. In addition to a statistically secured coefficient k, the following parameters influence the tensile resistance of composite dowels with PZ geometry (figure 7):

    - the width of the steel tooth b_{CD} or the distance of the load transferring contact points
    - the embedment depth of these contact points in the concrete h_{eff}
    - the concrete tensile strength, assumed via the square root of the characteristic compressive strength
    - the arrangement of the transversal reinforcement via the coefficient k_ρ

On the basis of tests, the coefficient k_ρ could be determined to 1.8 for adjacent transversal reinforcement bars or 1.2 for reinforcement bars outside the steel tooth undercut. The statistical evaluation leads to the equations given in Chapter 5. As a matter of fact, it has to be respected that due to the brittle tensile load-bearing behaviour no plastic force redistributions can be applied. Systematic tensile forces can therefore, at best, be transferred by one dowel, otherwise the elastic distribution of tensile forces over several dowels must be determined more precisely.

$$P_Z = k \cdot \left(\frac{\pi}{\tan\alpha \sin\alpha} + \frac{2 \cdot b_{CD}}{h_{eff} \cdot \sin\alpha}\right) \cdot h_{eff}^{1,5} \cdot \sqrt{f_{ck}} \cdot k_\rho$$

Figure 7. Determination of the pry-out cone geometry in case of one dowel or block failure and design approach.

4.3 Approach to consider the combined shear-tensile-resistance

In [29] an interaction relationship was proposed (figure 8) which divides both of the effecting shear and tensile forces by the corresponding resistances while each quotient was calibrated with an exponent k to consider the interaction relationship. On the basis of test results, the exponent k could be determined for different dowel geometries and reinforcement arrangements.
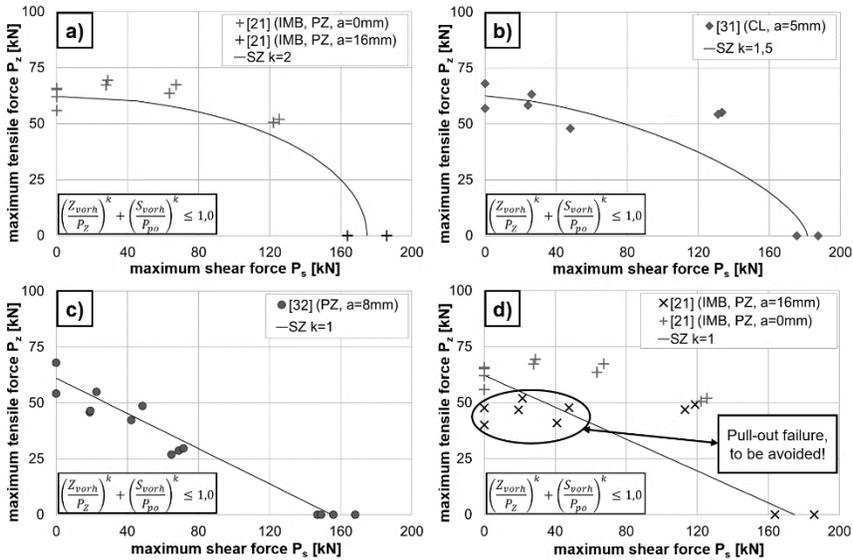

Figure 8. Shear-tensile-interaction relationships for reinforcement bars at the steel dowel (a), within the steel tooth undercut (b+c) and outside the steel tooth undercut (d).

Depending on the position of the transversal reinforcement, three cases can be distinguished. The maximum resistance under a combined shear-tensile load can be achieved if the transversal reinforcement is placed directly at the steel tooth within the undercut (a = 0 mm). In this case, the resulting shear-tension interaction curve can be seen in figure 8a and the exponent k can be set to 2.0. The diagram contains test results from [21]. If the transversal reinforcement does not contact the steel tooth but still is in the undercut area (figure 8b, a = 5 mm) with tests according to [31], the exponent k can be selected as 1.5 for the dowel geometries PZKL and CL, whereas in the case of the PZ geometry (figure 8c, a = 8 mm) with tests according to [32] an interaction coefficient of k = 1.0 must be used. If no explicit attention is paid to the arrangement of the transversal reinforcement, no tensile stress may be applied in the case of the PZ geometry, while with the CL and PZKL geometries still an interaction coefficient of k = 1.0 (figure 8d) with tests according to [21] can be applied. If systematic tensile forces occur, is important to ensure that the transversal reinforcement is positioned as close as possible to the steel tooth to increase the tensile resistance. The proposed interaction relationships have been further developed on the basis of the proposed models according to [33].

4.4 Approach to consider transversally cracked concrete slabs

In [34] an equation for the mechanical derivation of a reduction factor ψ_{crack} was developed which considers the concrete strength, the geometric conditions and the crack pattern. The influence of the crack pattern was very complex to determine due to the mechanical consistency and was simplified in [35] with the help of conservative geometric assumptions. On the basis of a statistical evaluation of the extended database, the reduction coefficient was further developed and statistically verified. In the elaborated proposal according to [1] only the geometric value h_{po} (height of the pry-out cone), the crack width w_r and

the corresponding crack spacing s_r were considered. The coefficients α and β can be determined for the different dowel geometries on the basis of Table 1.

$$\psi_{crack} = \frac{s_r}{6 \cdot h_{po} + s_r} + \frac{\sqrt{h_{po}}}{a + \beta \cdot w_r} \leq 1.0 \tag{1}$$

Table 1: Coefficients for the calculation of ψ_{crack} depending on the dowel geometry.

	α	β
PZ and PZKL	9	22
CL	13	31

The reduction of the resistance calculated with the help of equation (1) provides very good agreement with the test results for a wide range of possible crack widths. An overview of the quotients of experimental and theoretical load-bearing capacities can be found in [36].

4.5 Approach to consider composite dowels positioned close to the surface

According to the mechanical model based on the observations of the small-size tests, a quasi-hydrostatic compressive stress zone occurs in front of the steel teeth in the area of the effective steel tooth height $h_{d,eff}$ (figure 9) where the concrete is pulverized with increasing loads. The state of equilibrium is maintained both by the transversal reinforcement passing through and by the surrounding concrete. According to [37], the pressure p within this zone relates anti-proportionally to the third root of the effective contact area $t \cdot h_{d,eff}$.
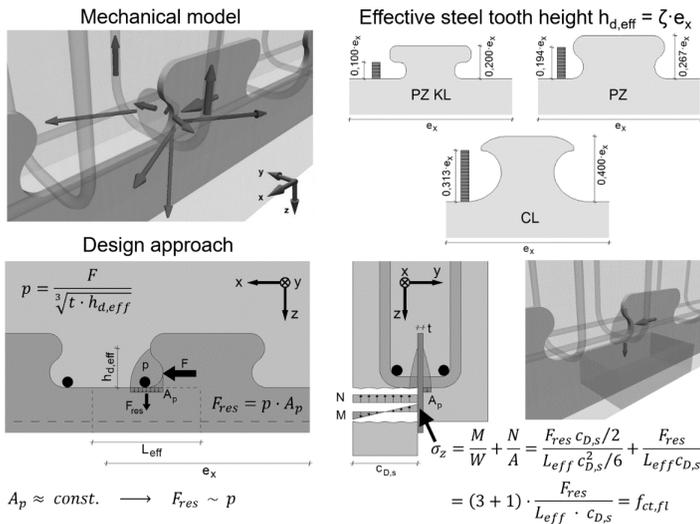

Figure 9. Schematic representation of the model assumptions for composite dowels positioned close to the surface.

The compressive stress zone causes, among other effects, a vertical force component F_{res}, which acts on an approximately constant and parameter-independent area A_p. Because of its eccentricity, it induces bending stresses within the concrete cover around the x-axis. If the concrete tensile stress σ_z locally reaches the flexural tensile strength $f_{ct,fl}$, the concrete edge spalls, the previously encased concrete powder escapes and the loss of load-bearing capacity is initiated. As a consequence, the resistance of composite dowels positioned close to the surface is significantly limited by maintaining the state of equilibrium of the quasi-hydrostatic compressive stress zone by the concrete cover. The resistance of this local zone can be approximated by applying static model assumptions as to be seen in figure 9.

4.6 Neglection of the failure mode 'shearing of the concrete dowel' in thin slabs

The current German approval additionally requires the calculation of the resistance against the failure mode shearing of the concrete dowel. As a matter of fact, when the required transversal reinforcement with an area of A ≥ 0.5·P/f_{sd} per dowel according to [8] is used, the failure mode has not been observed in tests with open dowel geometries and small embedment depth any more with regard to [12,34].

In addition, calculations for parameter configurations with PZ geometry showed that the failure mode shearing of the concrete dowel is not decisive in comparison to the failure mode pry-out for usual dimensions in building construction. Therefore, a design equation for determining the shear strength could be omitted for concrete covers below 100 mm in future regulations [21].

5   CONSISTENT DESIGN CONCEPT FOR COMPOSITE DOWELS

On the basis of the previously illustrated theoretical considerations, a consistent design model for composite dowels was developed which extends the scope of application of the current German approval [8]. For pure longitudinal shear loads, the characteristic value of the resistance per dowel $P_{S,Rk}$, considering the potential failure modes steel failure P_{pl}, pry-out of a concrete cone in non-cracked or transversely cracked concrete P_{po} and edge failure P_{poe}, is derived from the calculative minimum of the equations given in figure 10.

Shear resistance

$$P_{S,Rk} = \min \begin{cases} P_{pl,k} = \lambda_{geo} \cdot e_x \cdot t_w \cdot f_y & \rightarrow \quad \text{Steel failure} \\ P_{po,k} = k_1 \cdot \chi_x \cdot \chi_y \cdot h_{po}^{1,5} \cdot \sqrt{f_{ck}} \cdot (1 + \rho_{D,i}) \cdot \psi_{crack} & \rightarrow \quad \text{Pry-out} \\ P_{poe,k} = 2,16 \cdot \sqrt{f_{ck}} \cdot k \cdot c_{D,s} \cdot \sqrt[3]{t_w \cdot h_{d,eff}} \cdot \sqrt[3]{e_x} & \rightarrow \quad \text{Edge failure} \end{cases}$$

λ_{geo} specific geometry factor:
      $\lambda_{geo,PZ} = 0,286$; $\lambda_{geo,PZKL} = 0,186$; $\lambda_{geo,CL} = 0,259$

e_x steel tooth distance in [mm];
      150 mm ≤ e_x ≤ 500 mm

t_w thickness in [mm]; 4 mm < t_w ≤ 60 mm;
      maximum $t_{w,max}$ = 40 mm is used in the calculation

f_y nominal value of the steel yield strength in [N/mm²]

f_{ck} characteristic concrete compression strength in [N/mm²]

k_1 factor for failure mode pry-out:
      71 bei PZ- und PZKL-Geometrie
      95 bei CL-Geomerie

h_{po} height of the fictitious pry-out cone in [mm]

$h_{po,PZ} = \min \begin{cases} c_{D,o} + 0,07 \cdot e_x \\ c_{D,u} + 0,08 \cdot e_x \end{cases}$

$h_{po,PZKL} = \min \begin{cases} c_{D,o} + 0,05 \cdot e_x \\ c_{D,u} + 0,06 \cdot e_x \end{cases}$

$h_{po,CL} = \min \begin{cases} c_{D,o} + 0,07 \cdot e_x \\ c_{D,u} + 0,13 \cdot e_x \end{cases}$

$\rho_{D,i}$ reinforcement degree for failure mode pry-out : $\rho_{D,i} = \dfrac{E_s \cdot A_{sf}}{Ecm \cdot A_{D,i}}$

A_{sf} transversal reinforcement area in the concrete slab in [mm²]:
      $A_{sf} = A_b + A_t$

$A_{D,i}$ participating concrete area in [mm²]: $A_{D,i} = h_c \cdot e_x$

h_c height of the concrete slab in [mm]

E_s modulus of elasticity of the steel in [N/mm²]

E_{cm} modulus of elasticity of the concrete in [N/mm²]

$c_{D,o}$ upper concrete cover to the steel tooth in [mm]; $c_{D,o}$ ≥ 30 mm

$c_{D,u}$ lower concrete cover to the steel tooth in [mm]; $c_{D,u}$ ≥ 30 mm

$c_{D,s}$ lateral concrete cover to the steel tooth in [mm]; $c_{D,s}$ ≥ 45 mm

χ_x reduction factor with regard to e_x
      $\chi_x = 1,0$ for e_x ≥ 4,5·h_{po}
      $\chi_x = \dfrac{e_x}{4,5 \cdot h_{po}} ≤ 1,0$ for e_x < 4,5·h_{po}

χ_y reduction factor with regard to the number of composite dowel stripes, to e_x and to the transversal distance of the composite dowels e_y:
      in case of one composite dowel stripe:
      $\chi_y = 1,0$
      in case of two composite dowel stripes:
      $\chi_y = 1,0$ for e_y ≥ 9·h_{po}
      $\chi_y = \dfrac{1}{2} \cdot \left(\dfrac{e_y}{9 \cdot h_{po}} + 1 \right) ≤ 1,0$ for   120 mm < e_y < 9·h_{po}

ψ_{crack} reduction factor to consider transversal cracks:
      $\psi_{crack,PZ/PZKL} = \dfrac{s_r}{6 \cdot h_{po} + s_r} + \dfrac{\sqrt{h_{po}}}{9 + 22 \cdot w_r} ≤ 1,0$
      $\psi_{crack,CL} = \dfrac{s_r}{6 \cdot h_{po} + s_r} + \dfrac{\sqrt{h_{po}}}{13 + 31 \cdot w_r} ≤ 1,0$

s_r distance between cracks in [mm]

w_r crack width in [mm]

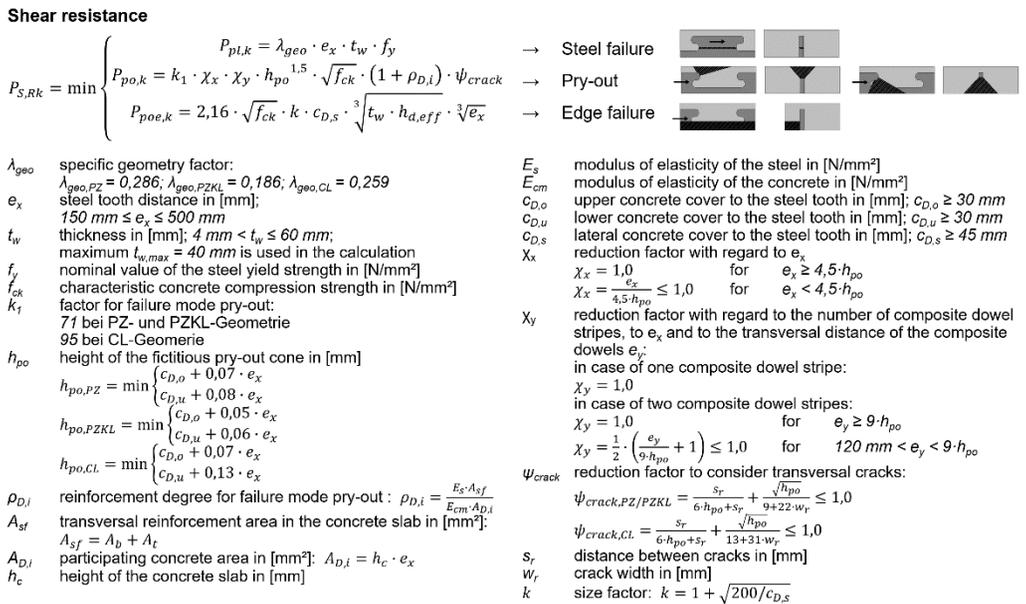k size factor: $k = 1 + \sqrt{200/c_{D,s}}$

Figure 10. Design equations for longitudinal shear resistance.

In the case of pure tensile loads, the characteristic value of the resistance per dowel $P_{Z,Rk}$ can be determined in a simplified way with regard to the pry-out failure mode, using the equations shown in figure 11 depending on the arrangement of the transversal reinforcement. If the transversal reinforcement contacts the steel tooth within its undercut, an increased tensile resistance can be applied. First of all, it has to be checked whether the effecting tensile force can be transferred by a single dowel. If this is not the case, the elastic distribution of the tensile force over several dowels must be determined more precisely. Then both the tensile resistance of each individual dowel and the block failure, which can be calculated by using b_{CD} as the distance between the outer load transferring areas of several dowels under tension, have to be considered. A plastic distribution of the tensile forces must not be assumed due to the low ductility.

Tensile resistance

$$P_{Z,Rk} = (7 + 2 \cdot \frac{b_{CD}}{h_{eff}}) \cdot h_{eff}^{1,5} \cdot \sqrt{f_{ck}} \quad \rightarrow \text{reinforcement in border position}$$

$$P_{Z,Rk} = (10,5 + 3,1 \cdot \frac{b_{CD}}{h_{eff}}) \cdot h_{eff}^{1,5} \cdot \sqrt{f_{ck}} \quad \rightarrow \text{reinforcement in steel undercut}$$

b_{CD} opening width between the steel teeth in [mm]
h_{eff} effective height of the pry-out cone in [mm]
f_{ck} characteristic concrete strength in [N/mm²]

Combined shear-tension resistance

$$\left(\frac{Z_e}{P_{Z,Rd}}\right)^k + \left(\frac{S_e}{P_{po,Rd}}\right)^k \leq 1,0$$

Z_e effecting tensile load in [kN]
$P_{Z,Rd}$ tensile resistance in [kN]
S_e effecting shear load in [kN]
$P_{po,Rd}$ shear resistance against pry-out in [kN]
k interaction factor [-]

reinforcement positions	k-factor		
	PZ	PZKL	CL
	invalid	1,0	1,0
	1,0	1,5	1,5
	2,0	2,0	2,0

Figure 11. Design equations for tensile- and shear-tensile-resistance.

Applications with composite dowels under tensile loads in cracked concrete shall be avoided as far as possible. Otherwise the transversal reinforcement must be placed closely to the steel tooth in the undercut and the crack width must be limited to $w_r = 0.1$ mm according to the current technical regulations. In addition, dowel geometries with a larger undercut (CL or PZKL) should be selected preferably. For composite dowels with PZ geometry, the design value of the calculated tensile resistance shall be reduced to 50% of the tensile resistance according to figure 11, for CL and PZKL geometry to 70%.

The equations to determine the resistance of composite dowels under combined shear-tensile loads are also given in figure 11, where the position of the transversal reinforcement has a decisive influence, too.

6   SUMMARY AND OUTLOOK

On the basis of numerous experimental investigations and corresponding numerical simulations, which were partly presented within this paper, and of former test results, a consistent design concept was developed to consider the tensile- as well as the shear-tensile-resistance of composite dowels, the influence of cracks and of positions close to the surface. This model approach shall form the basis for the preparation of a CEN Technical Specification, which can be introduced into the European standardization process and thus increase the competitiveness of composite dowels.

ACKNOWLEDGEMENT

REFERENCES

[1] Claßen M., Gallwoszus J., Hegger J. et al., "Nachhaltigkeitsbewertung von Deckensystemen mit großen Spannweiten", *Bauingenieur,* 89(3), pp. 125-133, 2014.

[2] Heinemeyer S., Gallwoszus J., Hegger J., "Verbundträger mit Puzzleleisten und hochfesten Werkstoffen", *Stahlbau*, 81(8), pp. 595-603, 2012.

[3] Kopp M., Christou G., Stark A. et al, "Integriertes Deckensystem für den Stahl- und Verbundbau", *Stahlbau*, 87(2), pp. 136-148, 2018.

[4] Hegger J., Claßen M., Schaumann P. et al., "Entwicklung einer integrierten Verbunddecke für nachhaltige Stahlbauten", *Stahlbau*, 82(1), pp. 11-17, 2013.

[5] European Committee for Standardization, *Schweißen - Lichtbogenschweißen von metallischen Werkstoffen*, DIN EN ISO 14555:2010, Brussels, 2010.

[6] Heinemeyer S., *Zum Trag- und Verformungsverhalten von Verbundträgern aus ultrahochfestem Beton mit Verbundleisten,* Phd thesis, RWTH Aachen University, 2011.

[7] DIBt Deutsches Institut für Bautechnik, *Allgemeine Bauartgenehmigung: Stahlverbundträger mit Verbunddübelleisten in Klothoiden- und Puzzleform*, German technical approval Z-26.1-23, Berlin, 2018.

[8] European Committee for Standardization, *Eurocode 4: Design of composite steel and concrete structures - Part 1-1: General rules and rules for buildings*, EN 1994-1-1:2004 + AC:2009, Brussels, 2004.

[9] Claßen M., Herbrand M., Stark A., "Dübelkennlinien von Verbunddübelleisten mit Stahlversagen", *Bauingenieur*, 92(6), pp. 237-244, 2017.

[10] Claßen M., Bielak J., Hürth D., "Verbunddübelleisten mit Betonausbruchversagen unter Zug- bzw. Druckbeanspruchung - Teil 1: Finite-Elemente-Analyse", *Beton- und Stahlbetonbau*, 113(5), pp. 348-359, 2018.

[11] Claßen M., Schmidt P., Wieneke K., "Verbunddübelleisten mit Betonausbruchversagen unter Zug- bzw. Druckbeanspruchung – Teil 2: Datenbank und Bemessungsansätze", *Beton- und Stahlbetonbau*, 113(6), pp. 443-452, 2018.

[12] Kopp M., Wolters K., Claßen M., Hegger J., Gündel M., Gallwoszus J., Heinemeyer S. and Feldmann M., "Composite dowels as shear connectors for composite beams – Background to the design concept for static loading", *Journal of Constructional Steel Research*, 147, pp. 488-503, 2018.

[13] Wolters K., Christou G., Feldmann M., "Untersuchungen zum Risswachstum in Verbunddübelleisten", *Bauingenieur*, 94(6), pp. 216-227, 2016.

[14] Gallwoszus J., *Zur Ermüdung von Verbundkonstruktionen mit Verbunddübelleisten,* Phd thesis, RWTH Aachen University, 2014.

[15] Christou G., Hegger J., Claßen M., "Fatigue of clothoid shaped rib shear connectors", *Journal of Constructional Steel Research*, 171, pp. 106-133, 2020.

[16] Christou G., Ungermann J., Wolters K. et al., "Ermüdung von Verbunddübelleisten", *Beton- und Stahlbetonbau*, 115(5), pp. 355-363, 2020.

[17] Christou G., Ungermann J., Wolters K. et al., "Ermüdung von Verbunddübelleisten – experimentelle Untersuchungen", *Stahlbau,* 89(4), pp. 388-398, 2020.

[18] Broschart Y. and Kurz W., "Tragverhalten von Verbundträgern mit randnahen Verbunddübelleisten", *Stahlbau*, 88(9), 2019.

[19] Broschart Y., Kurz W., Wolters K. et al., "Einflussfaktoren auf das Tragverhalten randnaher Verbunddübelleisten", *Bauingenieur*, 94(6), pp. 199-205, 2019.

[20] Christou G., Wolters K. and Broschart Y., "Verbunddübelleisten unter kombinierter Schub-Zug-Beanspruchung im gerissenen Beton", *Bauingenieur*, 94(6), pp. 228-236, 2019.

[21] Feldmann M., Wolters K., Hegger J., Claßen M, Christou G., Kurz W. and Broschart Y., "Konsistentes Bemessungsmodell für fertigungsoptimierte Verbunddübelleisten", Final report P1208, 2021.

[22] Claßen M., Hegger J., "Ausstanzmodell mit Rissreibung für Verbunddübelleisten im gerissenen Beton", *Beton- und Stahlbetonbau*, 112(3), pp. 155-166, (2017).

[23] Claßen M., Hegger J., "Ausstanzen von Verbunddübelleisten im gerissenen Beton", *Stahlbau*, 86(3), pp. 256-268, 2017.

[24] Claßen M., Gallwoszus J., Hegger J., "Einfluss von Querrissen auf das Schubtragverhalten von Verbunddübelleisten in schlanken Betongurten", *Beton- und Stahlbetonbau*, 109(12), pp. 882-894, 2014.

[25] Claßen M., Hegger J., "Anchorage of composite dowels", *Steel Construction*, 9(2), pp. 138-150, 2016.

[26] Claßen M., Hegger J., "Verankerungsverhalten von Verbunddübelleisten in schlanken Betongurten", *Bautechnik*, 91(12), pp. 869-883, 2014.

[27] Claßen M., Kurz W., Schäfer M. et al., "A mechanical design model for steel and concrete composite members with web openings", *Engineering Structures*, 197, 2019.

[28] Claßen M., Bielak J., Spelter A., "Verbundträger und Verbunddeckensysteme mit Stegöffnungen", *Stahlbau*, 88(7), pp. 685-697, 2019.

[29] Claßen M., Adam V., Kueres D. et al., "Zug-Schub-Interaktion von puzzleförmigen Verbunddübelleisten", *Beton- und Stahlbetonbau*, 112(6), pp. 334-345, 2017.

[30] European Committee for Standardization, *Eurocode 0: Grundlagen der Tragwerksplanung*, DIN EN 1990:2010-12, Brussels, 2010.

[31] Feldmann M., Kopp M., Hegger J. et al., *Endbericht P 1097 - Praxisreifes, integriertes Deckensystem für den Stahl- und Verbundbau*, Düsseldorf, 2017.

[32] Claßen M., *Zum Trag- und Verformungsverhalten von Verbundträgern mit Verbunddübelleisten und großen Stegöffnungen*, Phd thesis, RWTH Aachen University, 2016.

[33] Claßen M., Herbrand M., Adam V. et al., "Puzzle-shaped rib shear connectors subjected to combined shear and tension", *Journal of Constructional Steel Research*, 145, pp. 232-243, 2018.

[34] Claßen M., Hegger J., "Shear Tests on Composite Dowel Rib Connectors in Cracked Concrete", *ACI Structural Journal*, 115 (3), pp. 661-671, 2018.

[35] Claßen M.: "Vorschlag zur Erweiterung der Norm – Proposal for pry-out of composite dowels in cracked concrete", 2017.

[36] Wolters K., Christou G., Broschart Y., Claßen M., Feldmann M., Hegger J., Kurz W., "Entwicklung eines konsistenten Bemessungsmodells für Verbunddübelleisten", *Bauingenieur*, 2021.

[37] Eligehausen R., Mallée R., *Befestigungstechnik im Beton- und Mauerwerkbau*, Ernst & Sohn, Berlin, 2000.